

Electronic Supporting Information (ESI)

A new dioxo-molybdenum complex derived from amide based imine derivative for fluorescence recognition of Zr(IV) with phosphatase activity

Amit Kumar De,^a Tandrim Shaym,^a Subhasis Ghosh,^a Sunanda Dogra,^b Angshuman Roy Choudhury*^b and Debasis Das*^a

^aDepartment of Chemistry, The University of Burdwan, Burdwan-713104, WB, India.

^bDepartment of Chemical Sciences, Indian Institute of Science Education and Research (IISER), Mohali, Knowledge City, Sector 81, S.A.S. Nagar, Manauli P.O., Mohali, Punjab, India. 140306.

Materials

All experiments have been performed in aerobic conditions. High-purity PBS, 2,4-dihydroxybenzoic acid, thionyl chloride, hydrazine hydrate, *p*-nitrophenylphosphate (*p*NPP), and salicylaldehyde have been purchased from SigmaAldrich (India). On the other hand, molybdenum acetylacetonate [MoO₂(acac)₂], zirconium(IV) oxynitrate hydrate, [ZrO(NO₃)₂ · H₂O], and other metal nitrate salts have been purchased from Merck (India). Spectroscopic grade solvents have been used. All other chemicals are of analytical reagent grade and used without further purification. Milli-Q water (Milli-pore, 18.2 MΩ cm⁻¹) is used as and when required.

Instruments and measurements

Elemental analyses have been performed using Perkin Elmer 2400 (series-II) CHN analyzer. Shimadzu Multi Spec 2450 spectrophotometer is used for recording UV-Vis. spectra. FTIR spectra are recorded on a Shimadzu FTIR (model IR Prestige 21 CE) spectrophotometer. High-resolution mass spectra are captured using Xevo G2S/Q-Toff. microTM spectrometer. ¹HNMR and ¹³CNMR spectra are recorded using a Bruker Advance 400 (400 MHz) instrument using DMSO-d₆ solvent. The steady-state emission and excitation spectra are recorded by Hitachi F-7100 spectrofluorimeter using a quartz cell of 1 cm path length. Systronics digital pH meter (model 335) is used for pH measurement. Single crystal X-ray data have been collected at 200.0(2)K using a Rigaku XtaLabmini X-ray diffractometer using graphite-monochromated Mo-Kα radiation (0.71073Å) and Mercury CCD. CrysAlisPro 1.171.39.35c¹ was used for data collection, data

reduction, and empirical absorption correction. The crystal structure was solved using SHELXT², refined by full-matrix least-squares with SHELXL³ using the OLEX2⁴ suite. Images are generated using Mercury software.⁵

General method of UV-vis. and fluorescence titration

Stock solutions of **DBASL**, **DBASLM**, and $\text{ZrO}(\text{NO}_3)_2$ are prepared in EtOH-water (3:7, v/v) media. Working solutions are prepared from respective stock solutions by appropriate dilution. Fluorescence spectral data are collected using 2.5 nm \times 2.5 nm slit width.

Job's plot from fluorescence experiment: -

The sets of solutions bearing the probe **DBASLM** and analytes (ZrO^{2+}) were prepared in a way that the concentration of ligand and analyte in total remains constant (50 μM) in all the sets. The mole fraction (X) of analyte (ZrO^{2+}) is varied from 0.1 to 0.9 for the analyte **DBASLM**. The intensity of emissions ($\lambda_{\text{em}} = 477 \text{ nm}$, $\lambda_{\text{ex}} = 278 \text{ nm}$) was plotted as a function of the mole fraction of analytes. **DBASLM** forms a 1:1 (mole ratio) complex with ZrO^{2+} . These are approved by the corresponding mass spectra.

Determination of binding constant

The binding constants of **DBASLM** with ZrO^{2+} and **DBASL** with ZrO^{2+} are estimated through using a modified Benesi-Hildebrand equation⁶: $(F_{\text{max}} - F_0) / (F_x - F_0) = 1 + (1/K) (1/[C])^n$ where, F_{max} , F_0 and F_x are emission intensities for ligand in presence of analyte at saturation, in absence of analyte and at any intermediate analyte concentrations, respectively. A plot of $(F_{\text{max}} - F_0) / (F_x - F_0)$ vs. $[C]^{-1}$ (here, $n = 1.0$) gives the binding constant from the slope while $[C]$ is the molar concentration of analyte.

Calculation of detection limit

The detection limit (**DL**) may be predicted by the following equation⁷:

$$DL = \frac{3\sigma}{S}$$

σ is the standard deviation of the blank solution, and S is the slope of the calibration curve.

For the determination of standard deviation, the emission intensity of **DBASLM** and **DBASL** without any analyte (ZrO^{2+}) was replicated 10 times.⁸

Determination of rate constant of *p*-NPP hydrolysis.⁹

$$1/k_{\text{obsd}} = 1/k_1 + K/[S]$$

k_{obs} = Observed first-order rate constant at substrate concentration [S]

k_1 = Limiting rate constant (maximal observed rate) as [S] $\rightarrow \infty$

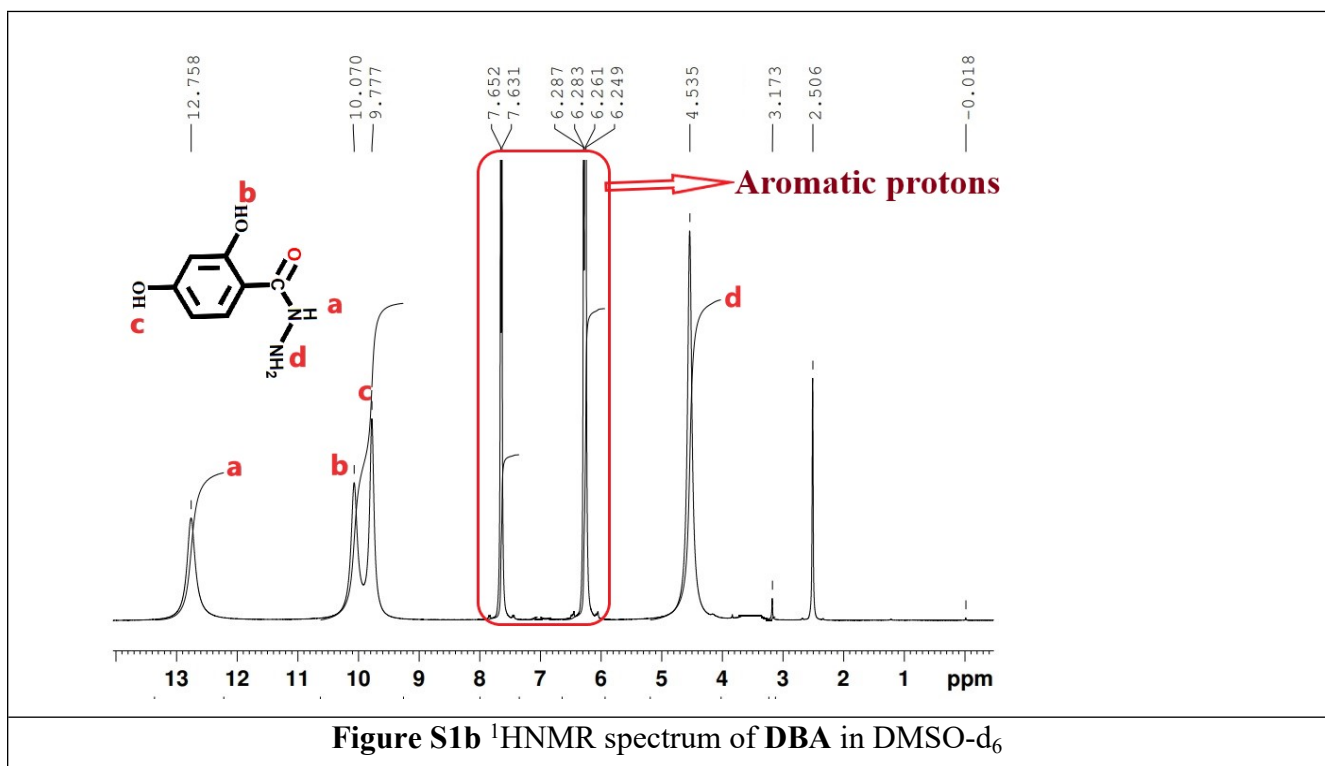
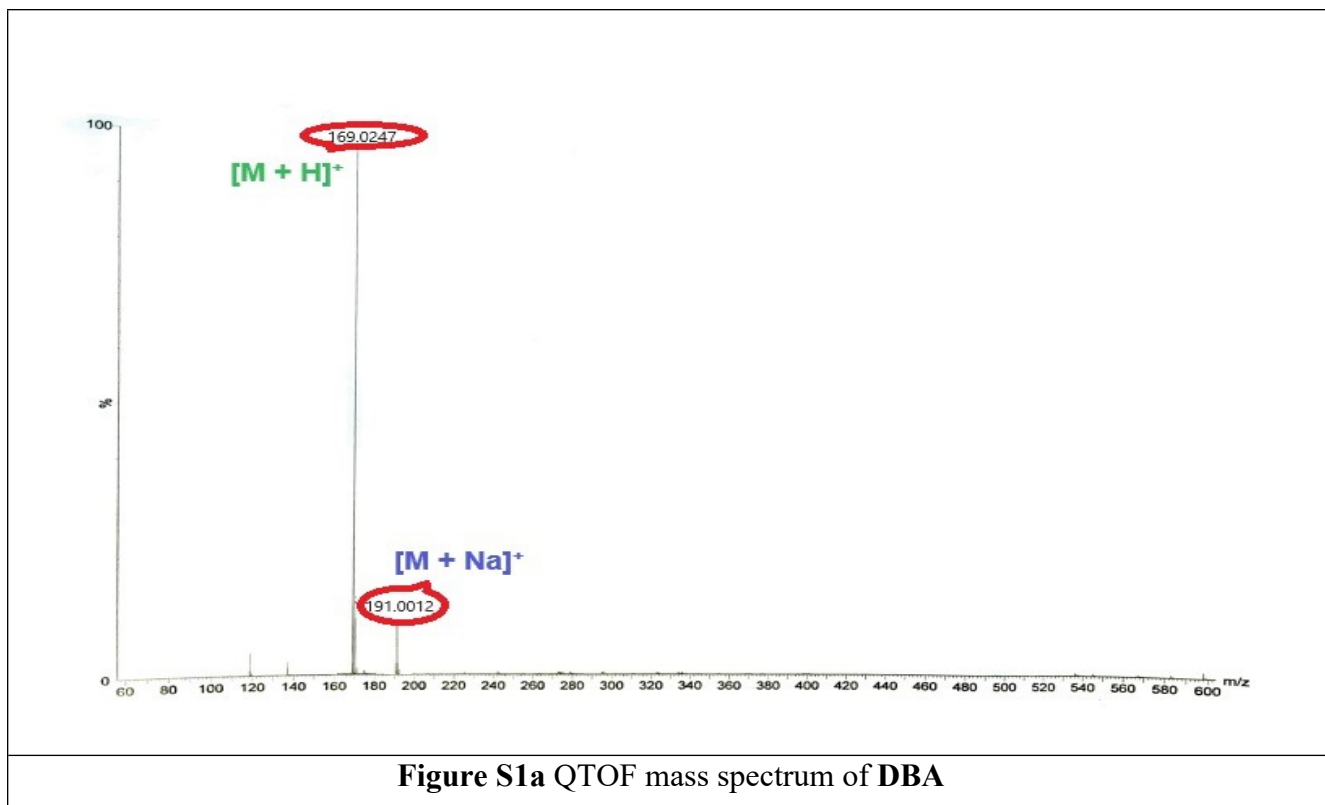
K = Constant related to substrate binding or equilibrium between species

[S] = Substrate concentration

Employing the equation, the plot of $1/k_{\text{obs}}$ vs. $1/[S]$ generates a linear plot that provides the value of k_1 .

References

1. CrysAlisPro 1.171.39.35c, User-Inspired Software for Single Crystal X-ray Diffractometers, Rigaku Oxford Diffraction, 2017, <https://rigaku.com/products/crystallography/x-ray-diffraction/crysalispro>
2. G. M. Sheldrick, *Acta Crystallogr., Sect. A: Found. Crystallogr.*, 2015, 71, 3–8.
3. G. M. Sheldrick, *Acta Crystallogr., Sect. C: Found. Crystallogr.*, 2015, 71, 3–8.
4. O. V. Dolomanov, L. J. Bourhis, R. J. Gildea, J. A. K. Howard and H. Puschmann, *J. Appl. Crystallogr.*, 2009, 42, 339–341.
5. C. F. Macrae, I. Sovago, S. J. Cottrell, P. T. A. Galek, P. McCabe, E. Pidcock, M. Platings, G. P. Shields, J. S. Stevens, M. Towler, and P. A. Wood. *J. Appl. Cryst.* 2020, 53(2), 226-235.
6. H. A. Benesi and J. H. Hildebrand, *J. Am. Chem. Soc.*, 1949, 71, 2703–2707.
7. M. Zhu, M. Yuan, X. Liu, J. Xu, J. Lv, C. Huang, H. Liu, Y. Li, S. Wang and D. Zhu, *Org. Lett.*, 2008, 10, 1481–1484.
8. S. Dey, R. Purkait, K. Pal, K. Jana and C. Sinha, *ACS Omega*, 2019, 4, 8451–8464.
9. A. J. Kirby and W. P. Jencks, *J. Am. Chem. Soc.*, 1965, 87, 3209–3216.



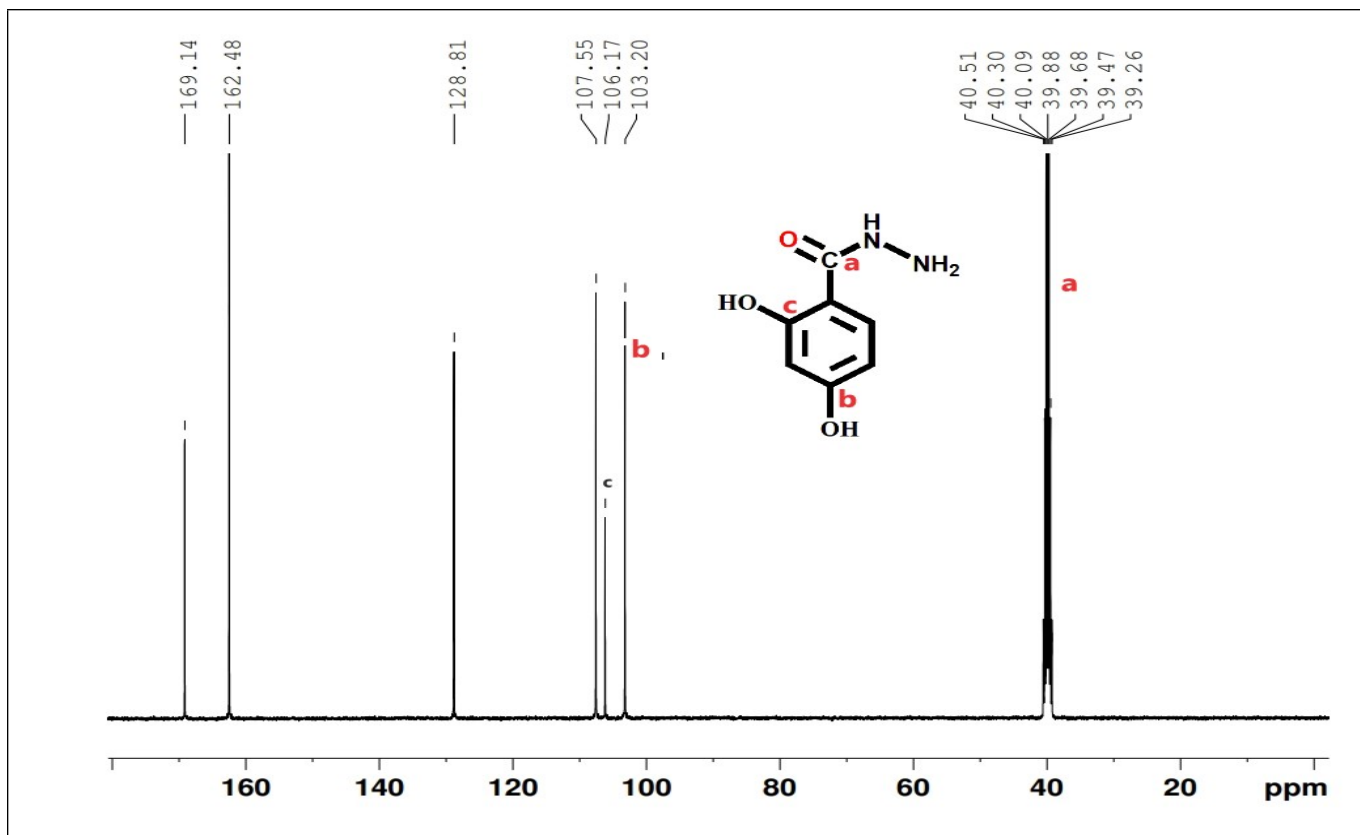


Figure S1c ^{13}C NMR spectrum of DBA in DMSO-d_6

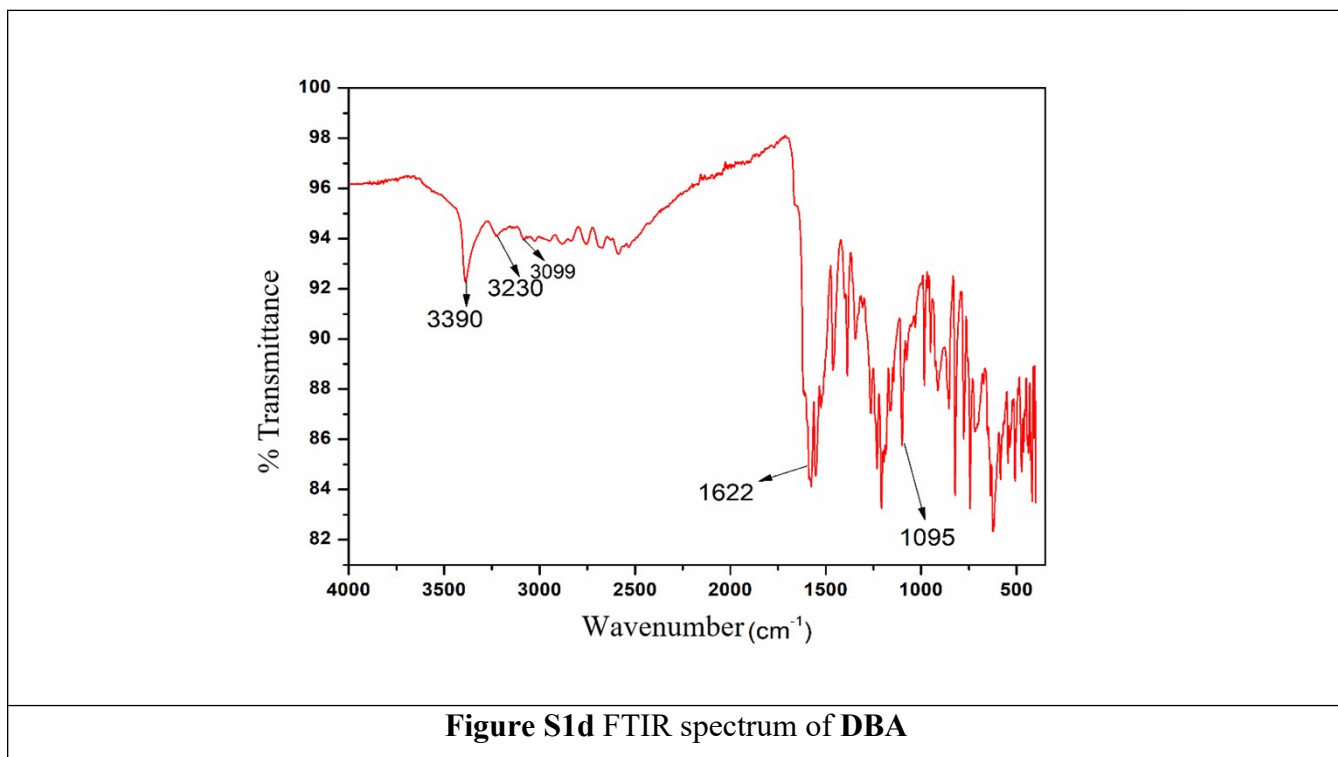
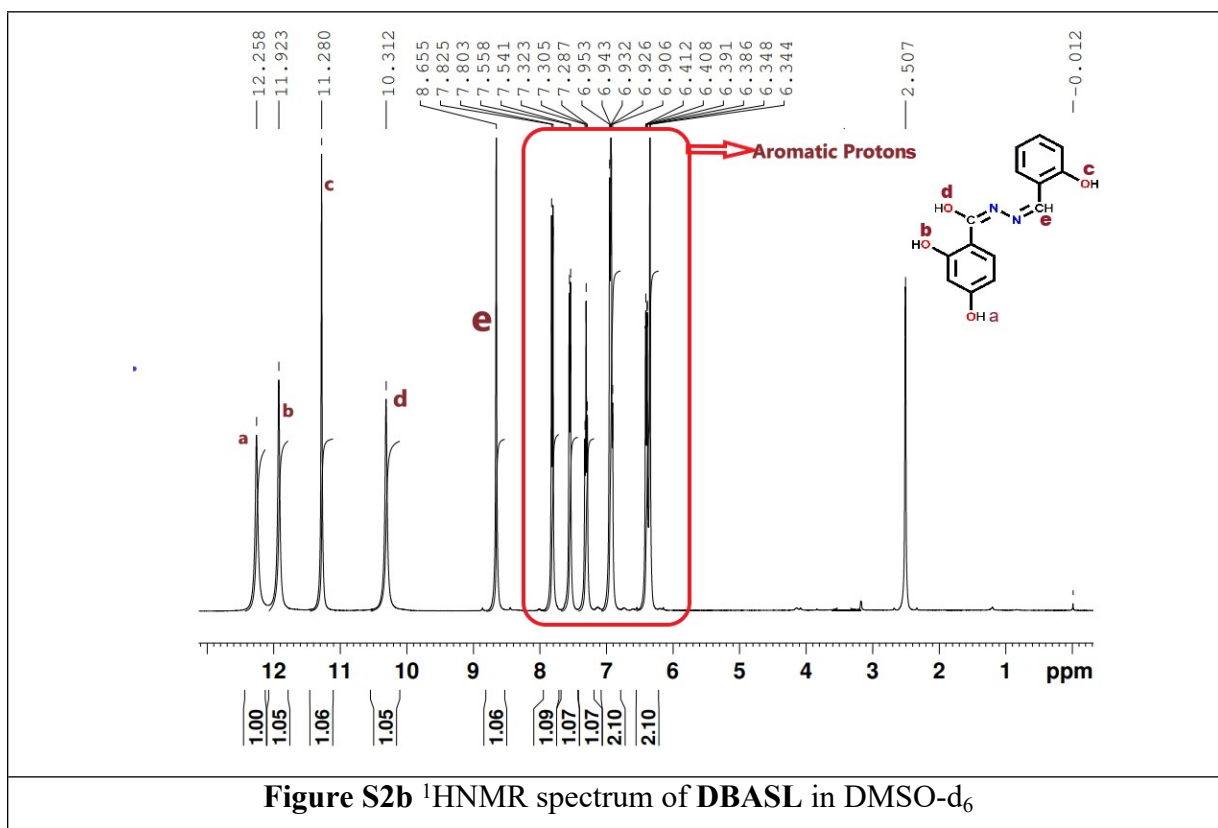
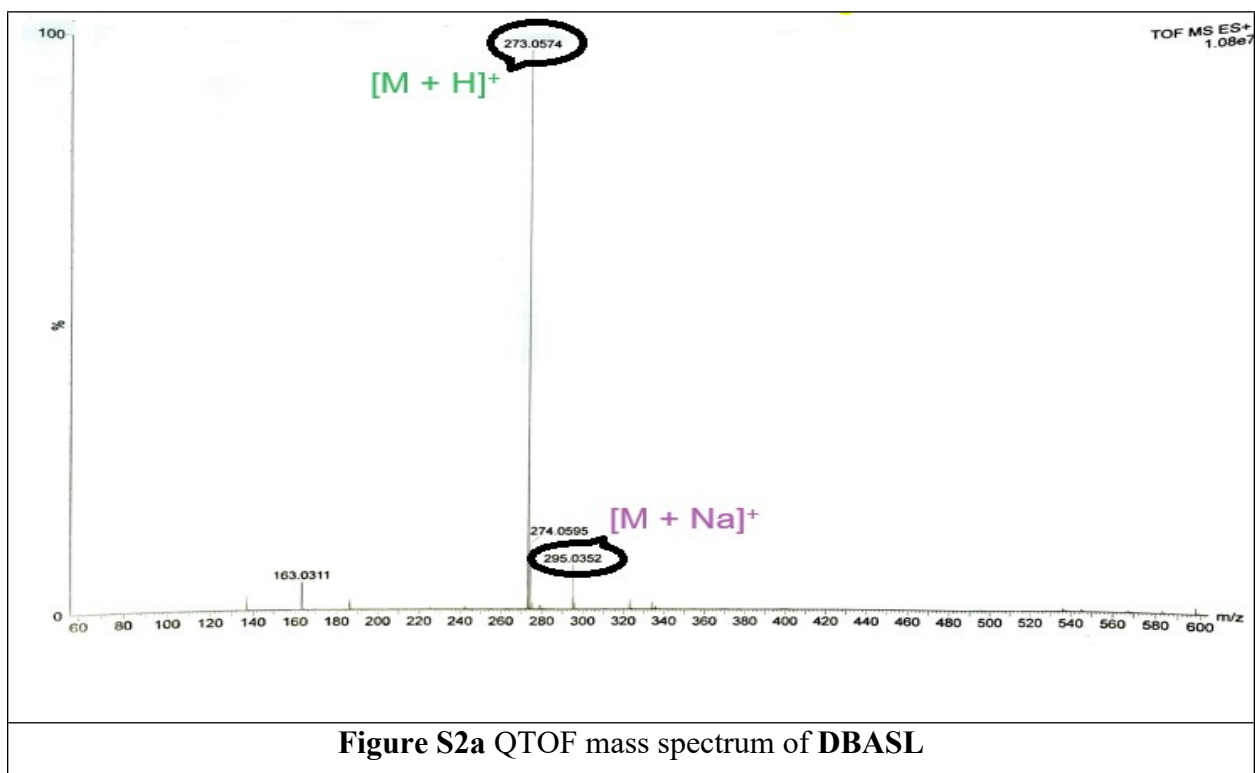


Figure S1d FTIR spectrum of DBA



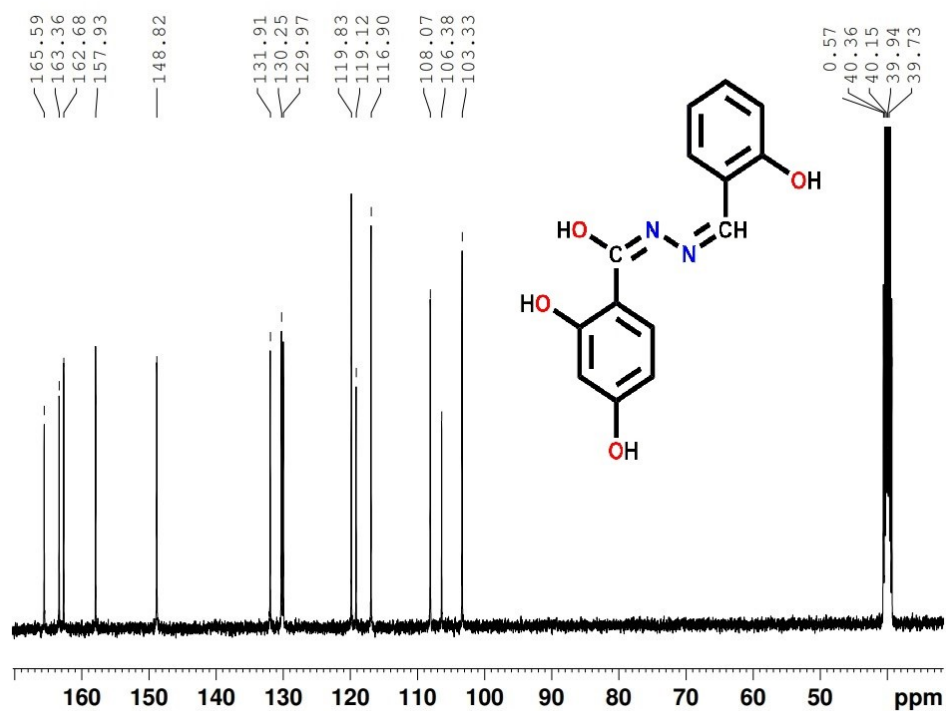


Figure S2c ^{13}C NMR spectrum of DBASL in DMSO-d_6

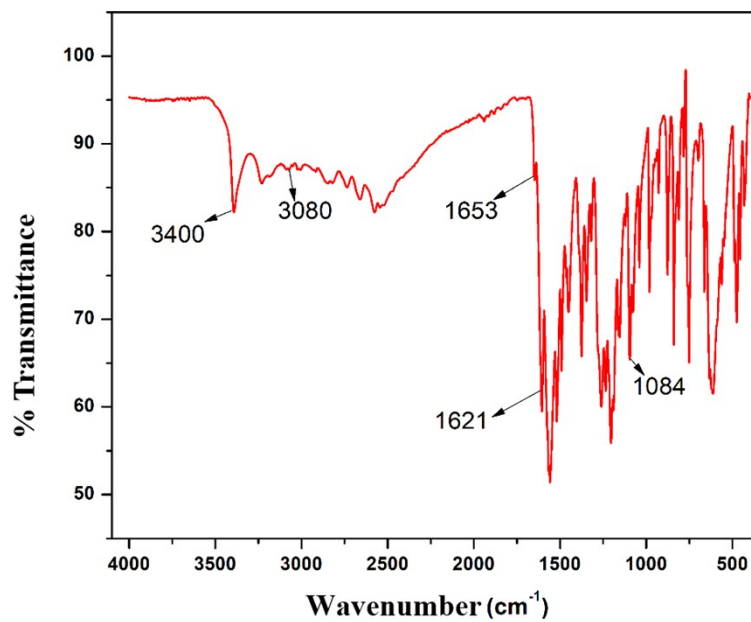


Figure S2d FTIR spectrum of DBASL

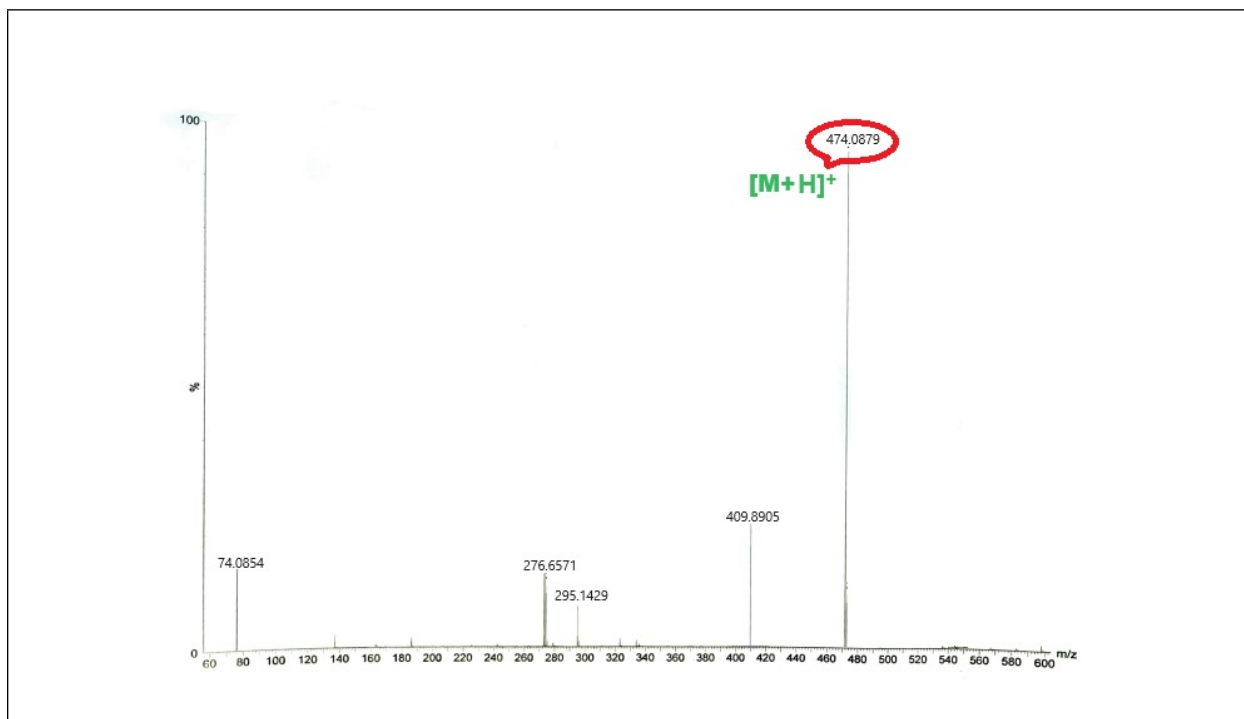


Figure S3a QTOF mass spectrum of **DBASLM**

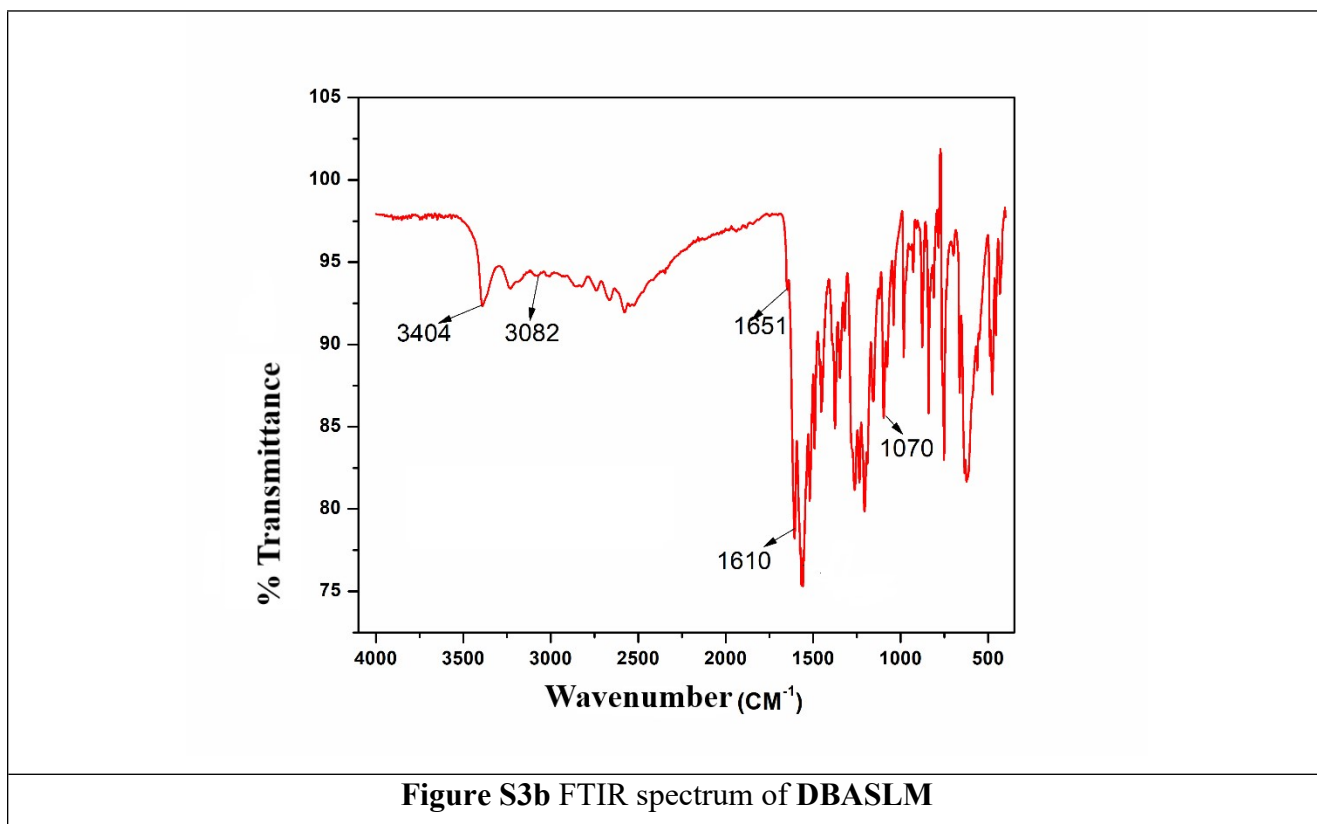


Figure S3b FTIR spectrum of **DBASLM**

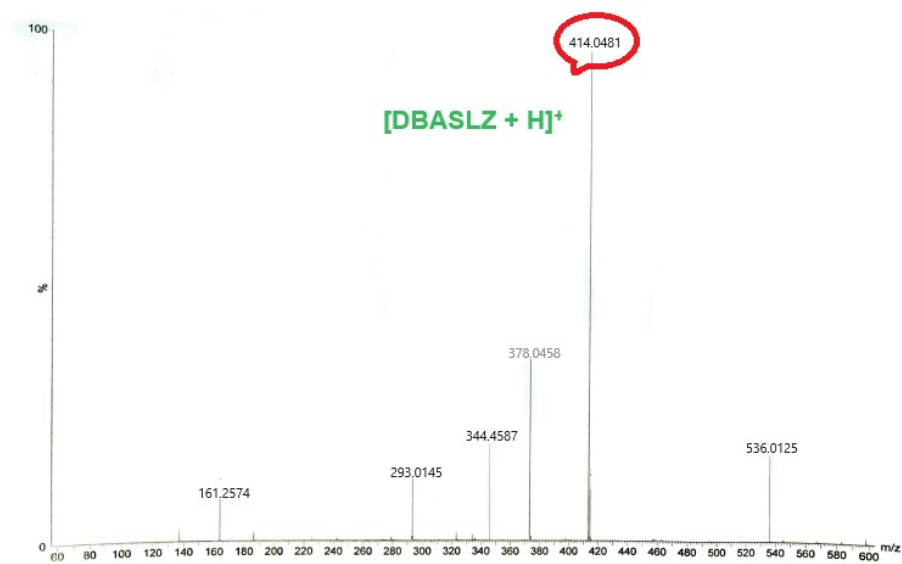


Figure S4a QTOF mass spectrum of DBASLZ

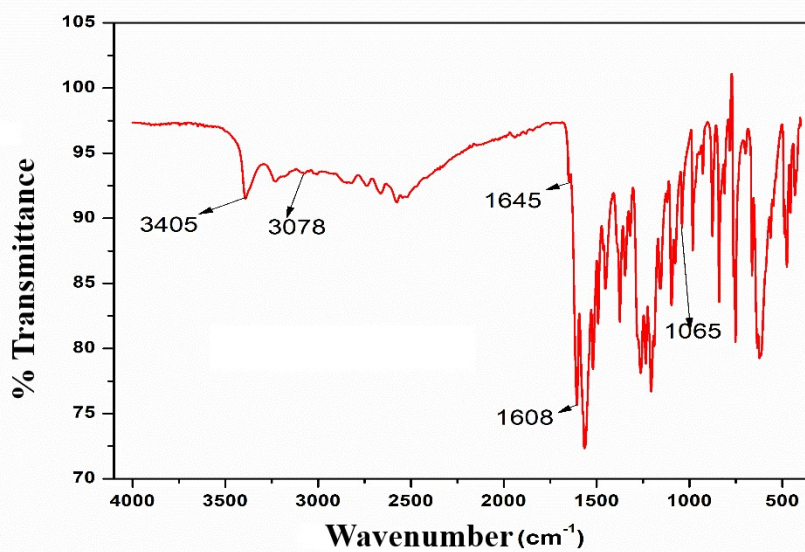


Figure S4b FTIR spectrum of DBASLZ

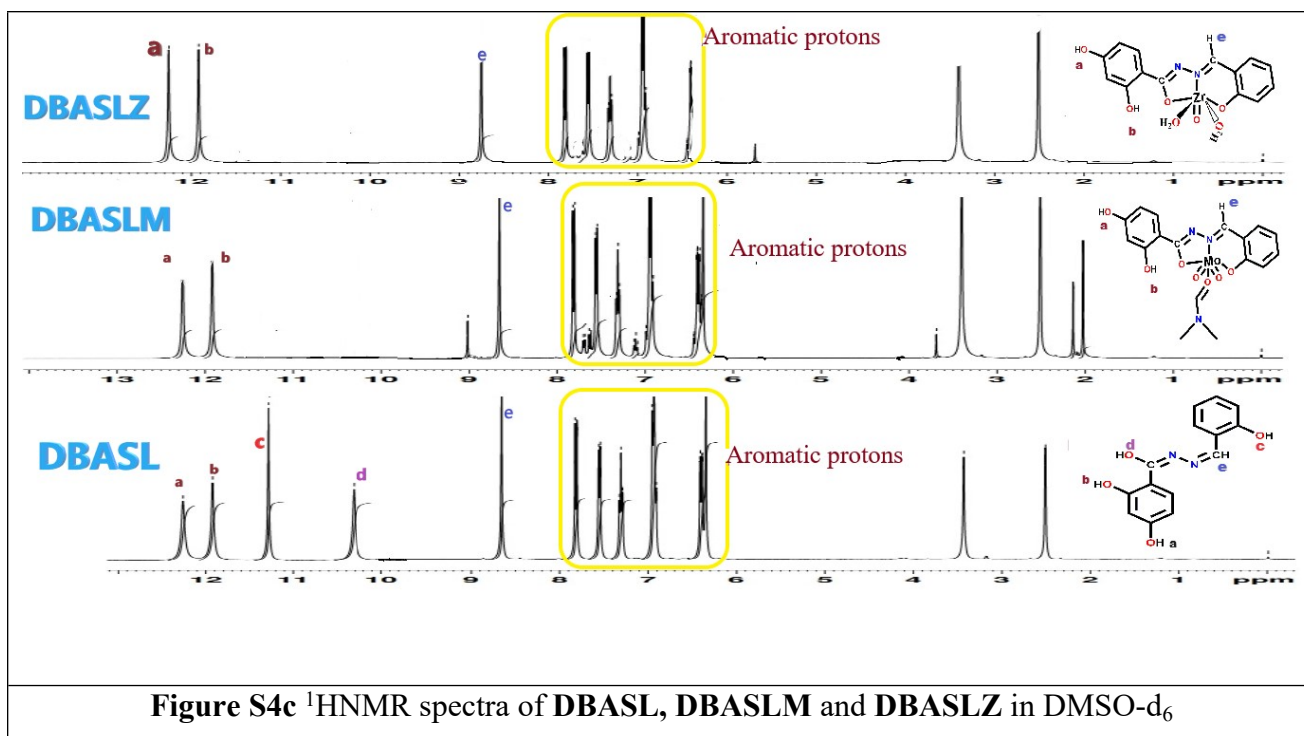


Figure S4c ^1H NMR spectra of **DBASL**, **DBASLM** and **DBASLZ** in DMSO- d_6

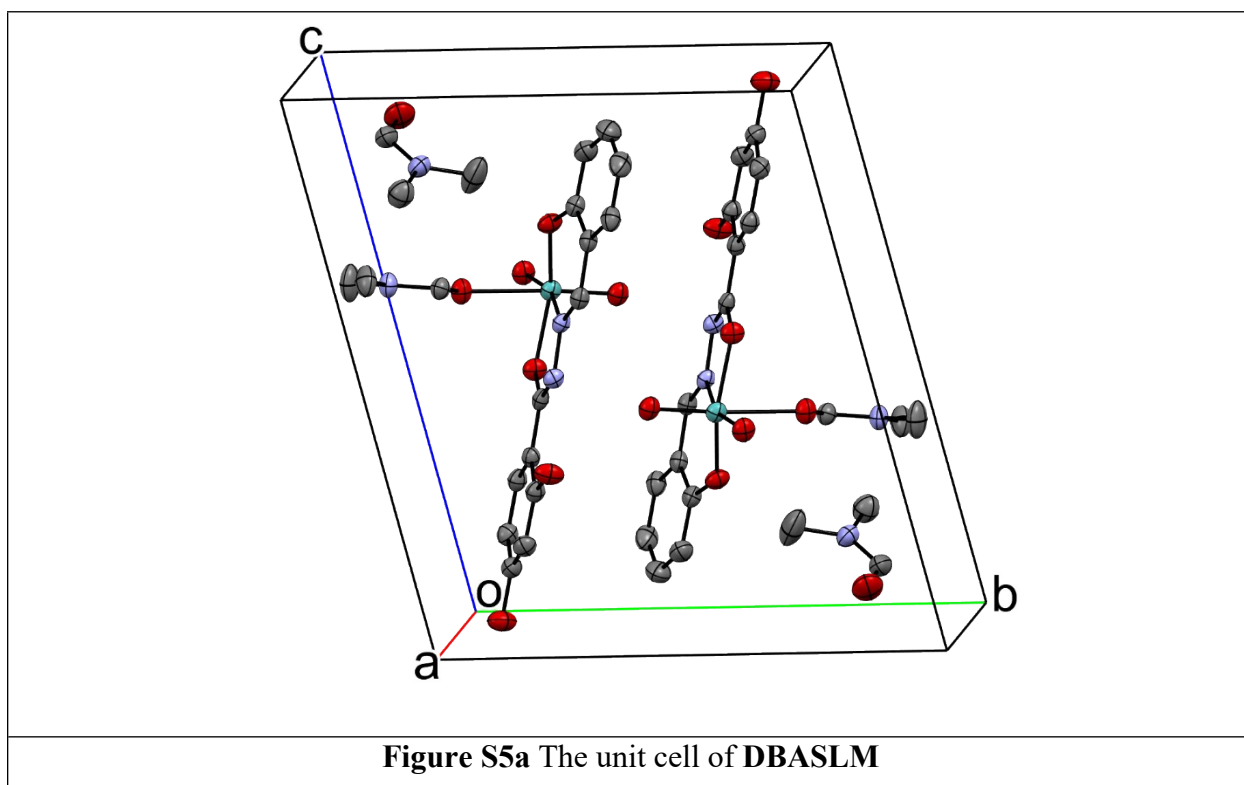


Figure S5a The unit cell of **DBASLM**

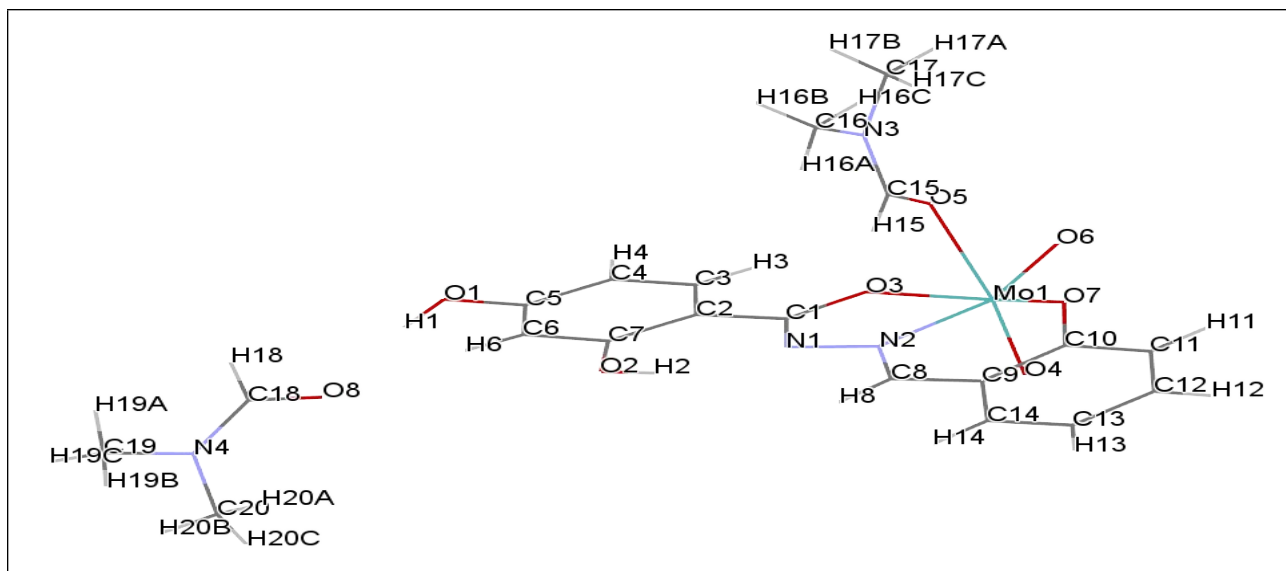


Figure S5b X-Ray crystallographic structure of DBASLM with labelling of atoms by wireframe model

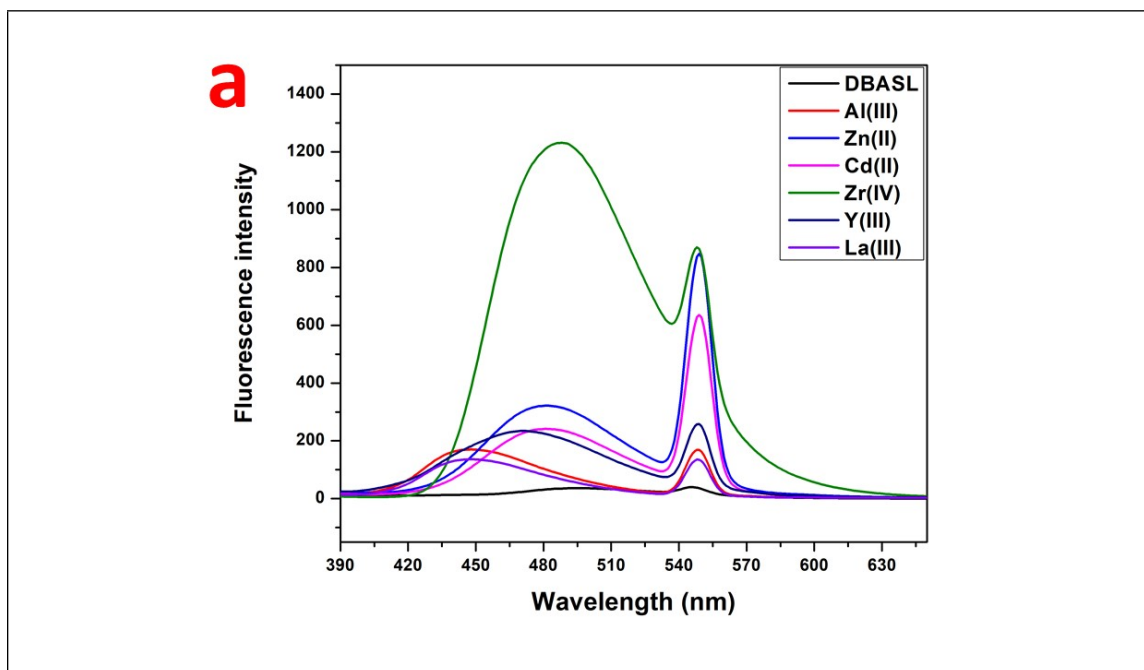


Figure S6a Emission intensity of BDASL (50 μM) in presence of common cations (50 μM each) in aqueous ethanol (1:1, v/v) ($\lambda_{\text{ex}} = 335 \text{ nm}$)

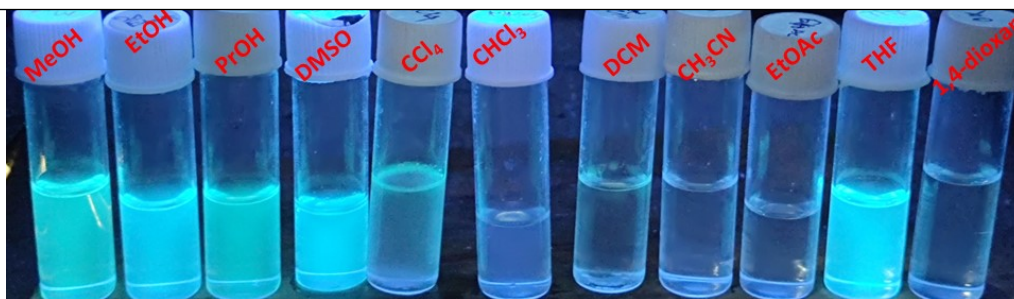


Figure S6b [DBASLM (60 μM) + ZrO^{2+} (100 μM) system]: colors under UV light in different solvents

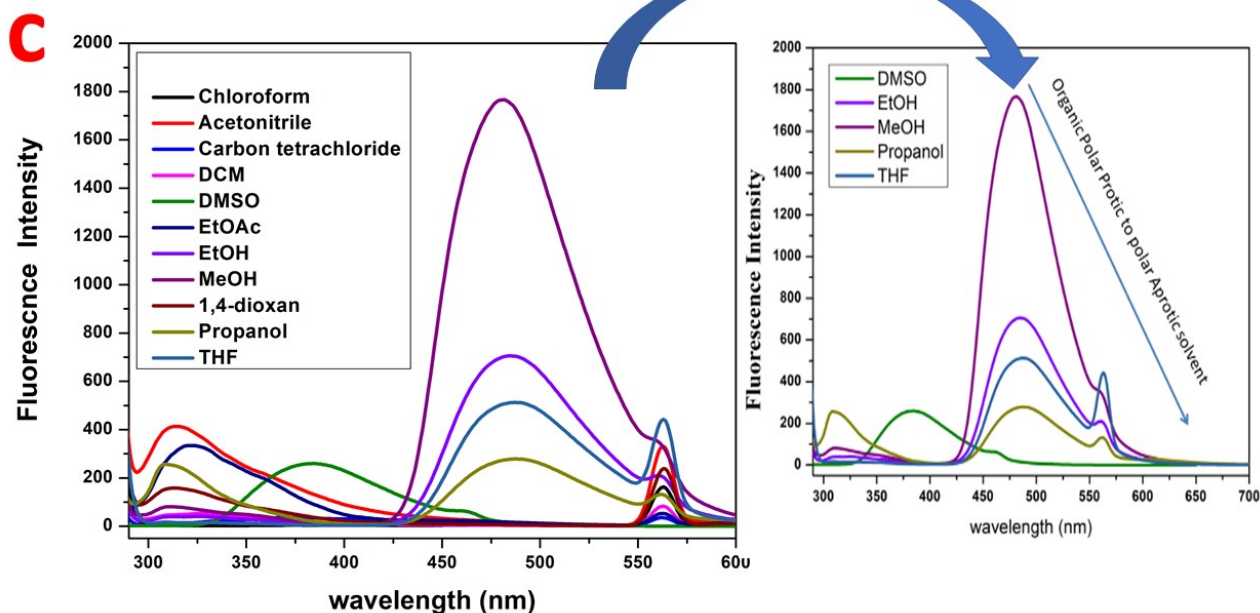


Figure S6c [DBASLM (60 μM) + ZrO^{2+} (100 μM) system]: effect of solvent on the emission spectra (left) and excitation wavelengths in protic and aprotic solvents (right). CCl_4 ($\lambda_{\text{ex}} = 272$ nm), CH_3CN ($\lambda_{\text{ex}} = 275$ nm), DCM ($\lambda_{\text{ex}} = 272$ nm), EtOAc ($\lambda_{\text{ex}} = 274$ nm), 1,4-dioxan ($\lambda_{\text{ex}} = 274$ nm), CCl_3 ($\lambda_{\text{ex}} = 271$ nm), EtOH ($\lambda_{\text{ex}} = 271$ nm), THF ($\lambda_{\text{ex}} = 270$ nm), propanol ($\lambda_{\text{ex}} = 275$ nm), DMSO ($\lambda_{\text{ex}} = 275$ nm) and MeOH ($\lambda_{\text{ex}} = 280$ nm).

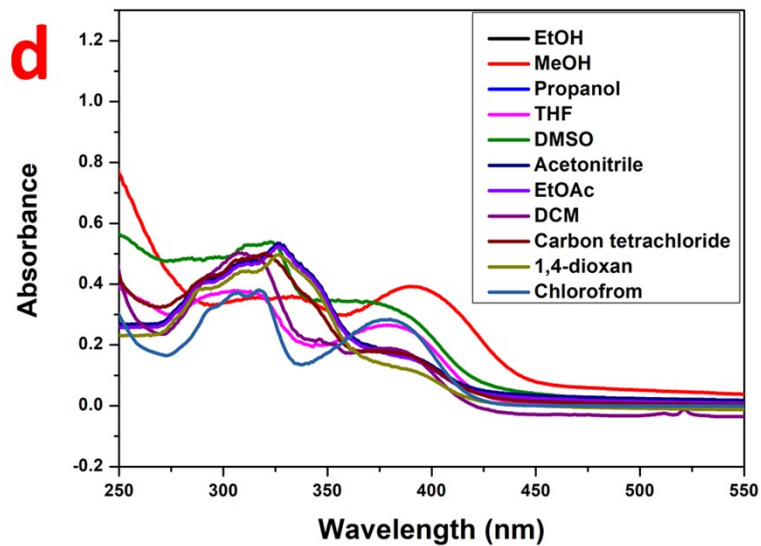
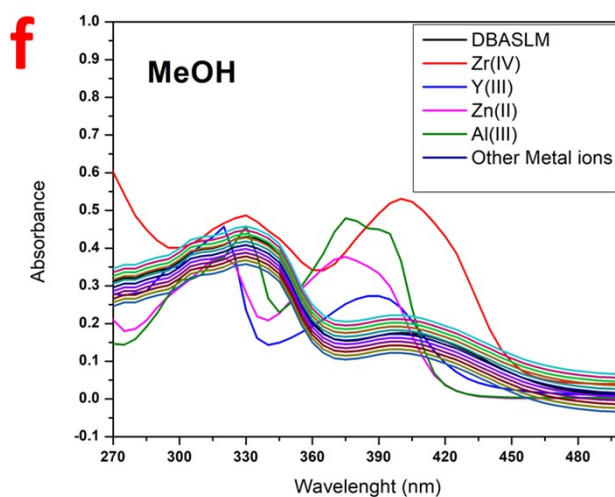
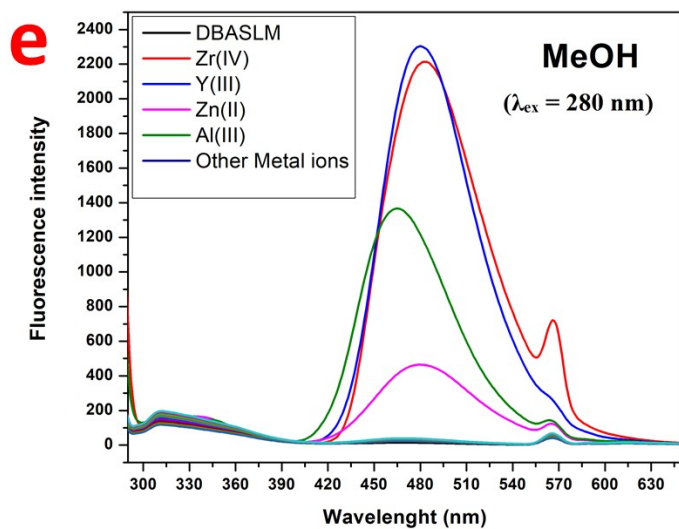
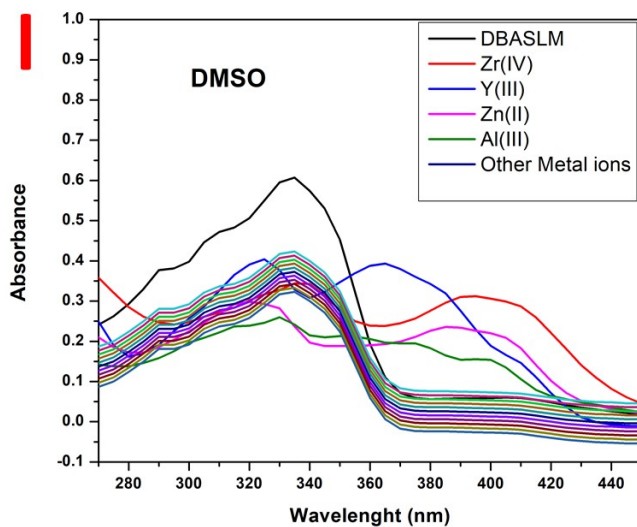
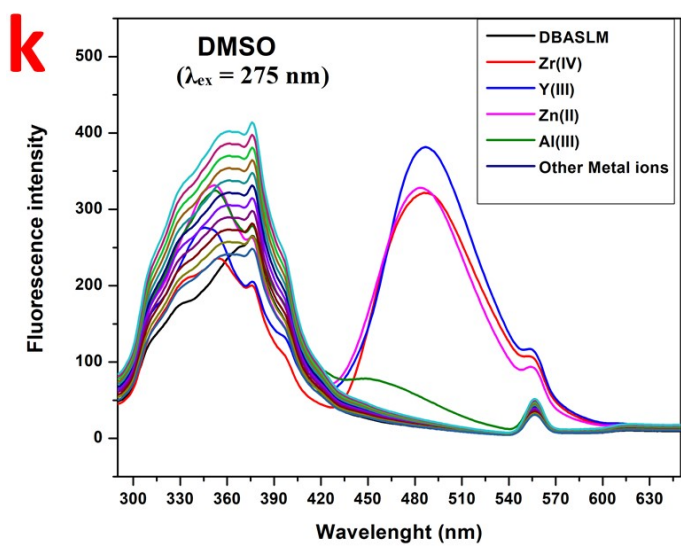
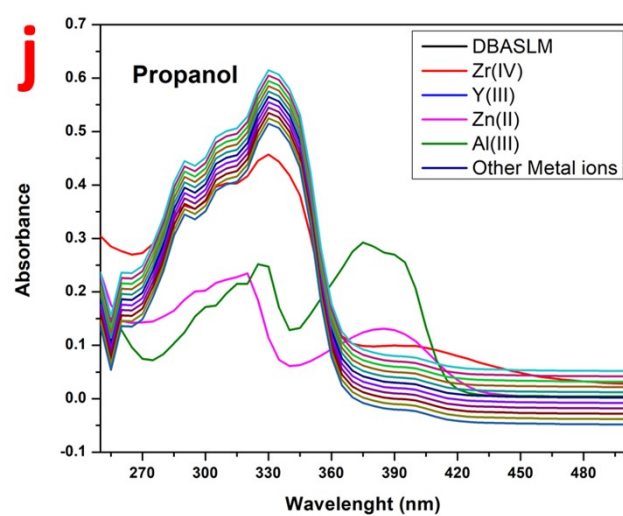
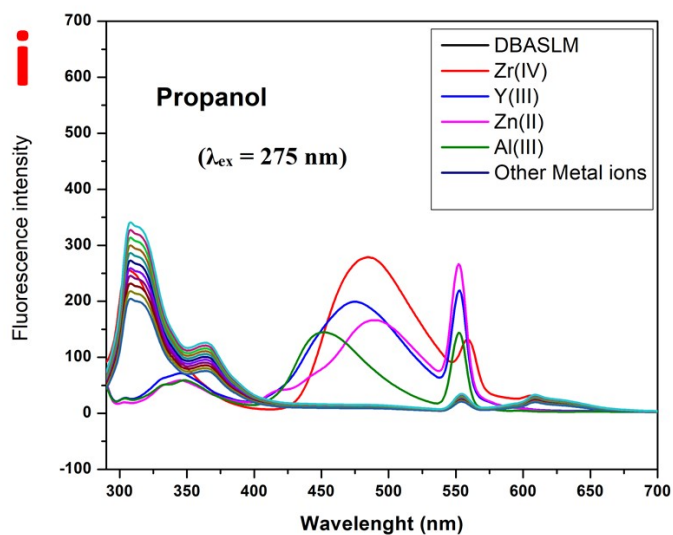
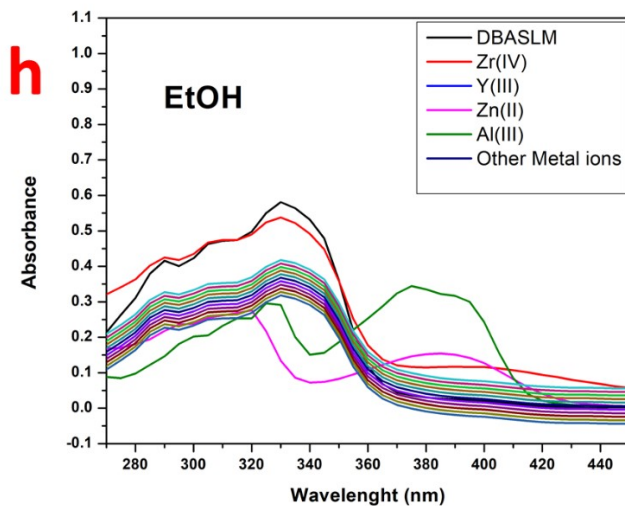
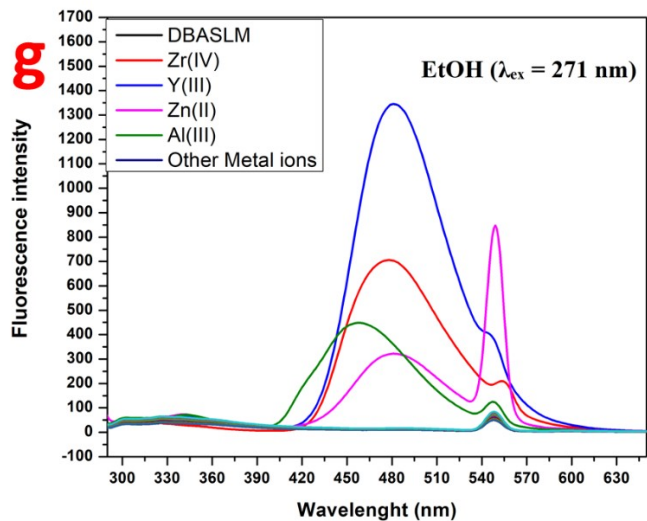
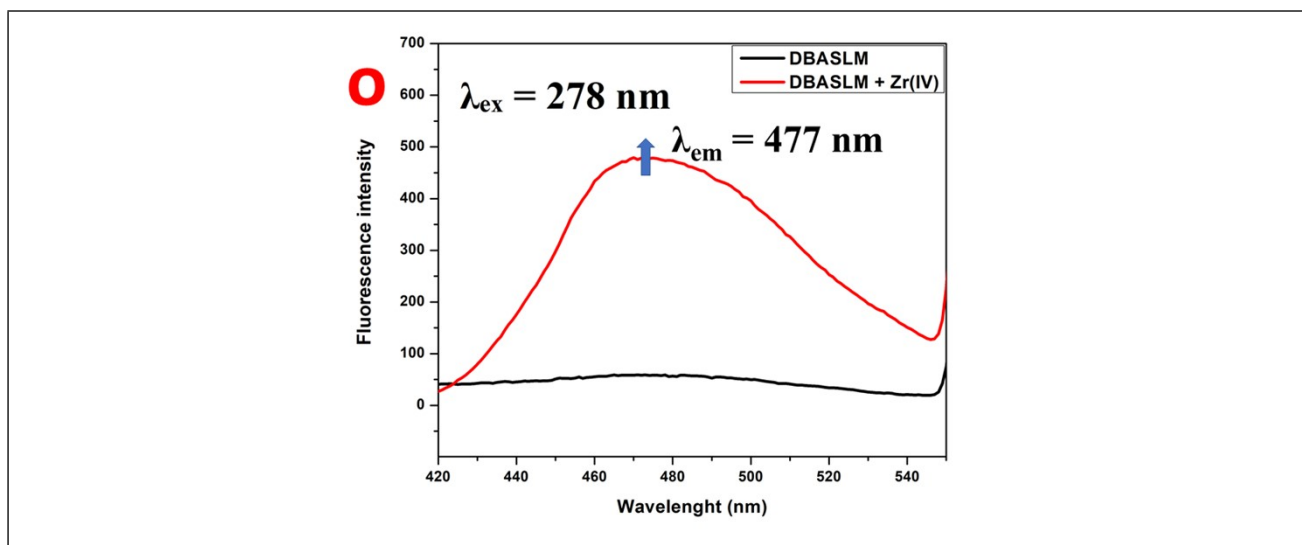
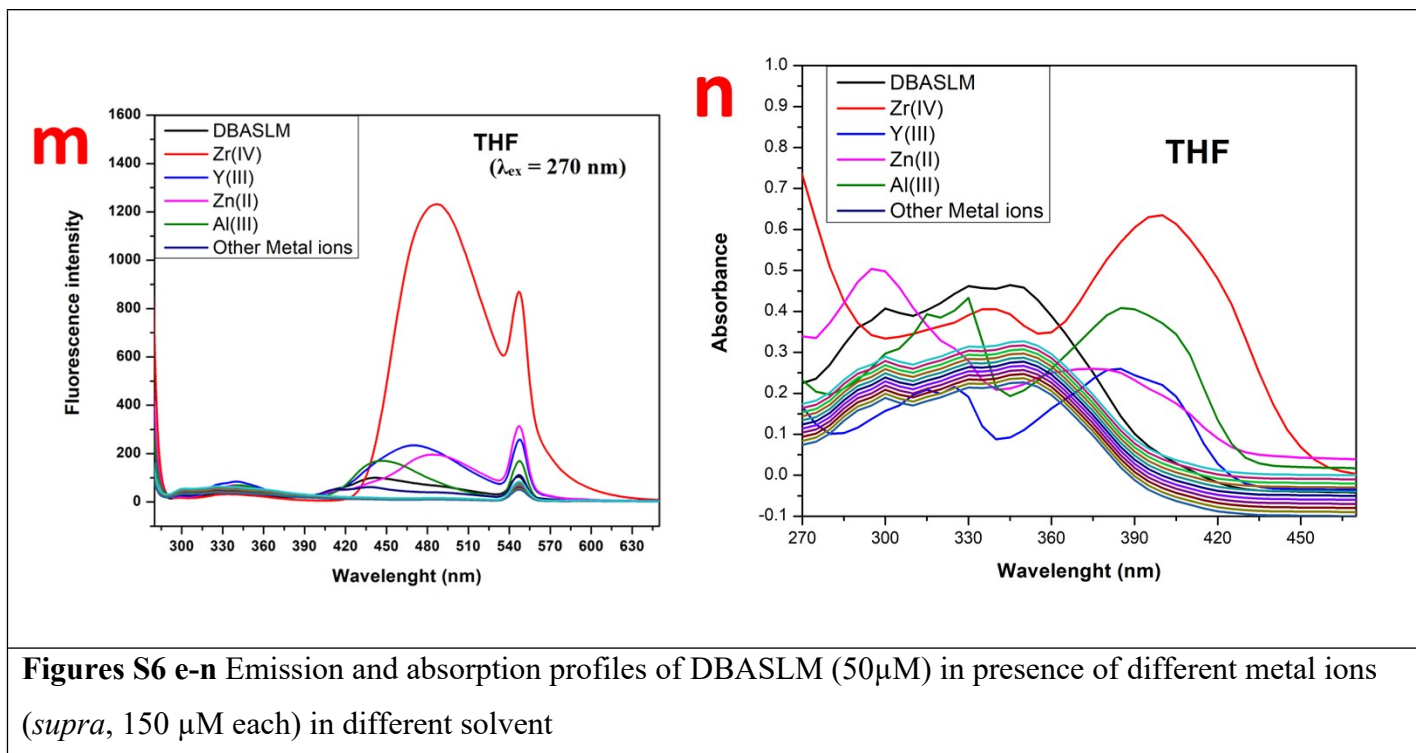
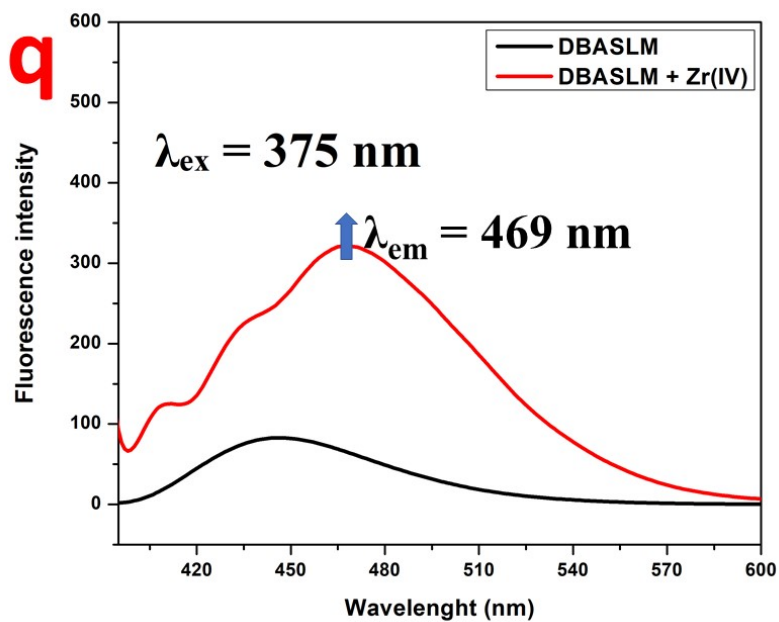
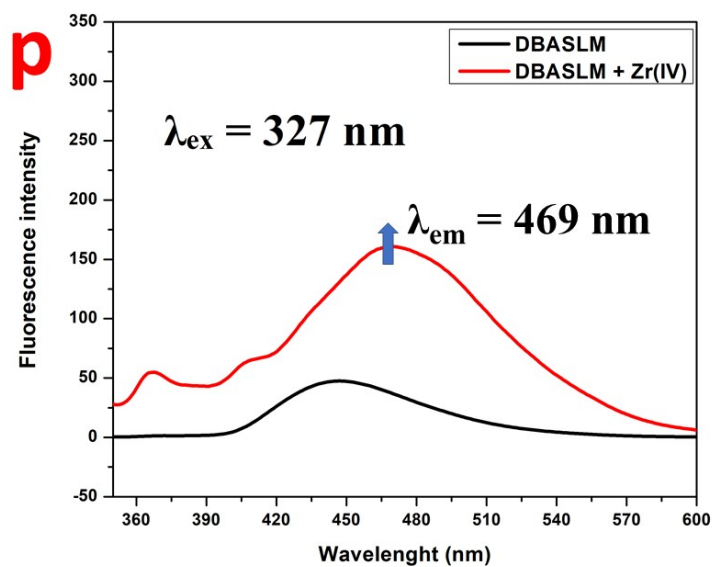


Figure S6d Effect of solvent on the absorption spectra of [DBASLM (60 μM) + ZrO₂⁺ (100 μM)] system









Figures S6 o-q Influence of different excitation wavelengths on the emission intensities of **DBASLM** (50 μM) and **DBASLM** (50 μM) + **ZrO²⁺** (150 μM) in ethanol-H₂O (3:7, v/v)

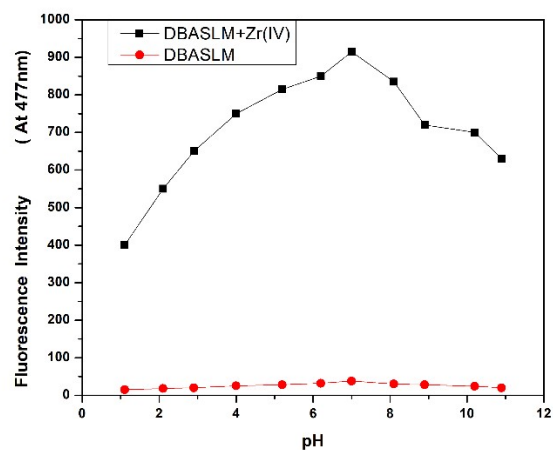


Figure S9 Changes in emission intensities of DBASLM vs. pH in presence and absence of ZrO^{2+} ($\lambda_{ex} = 278$ nm; $\lambda_{em} = 477$ nm, EtOH-H₂O (3:7, v/v)).

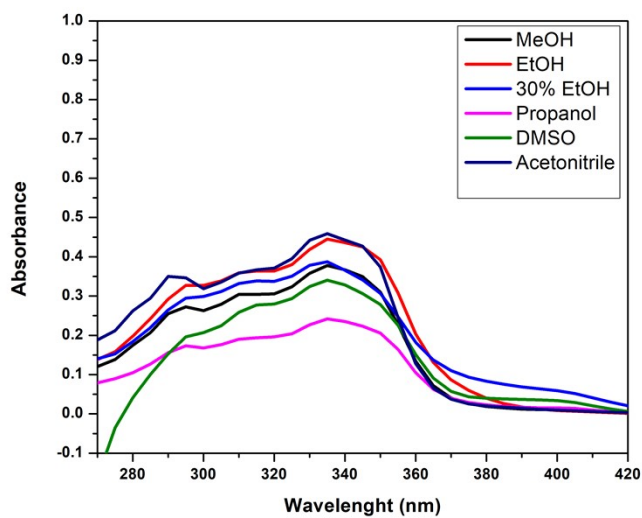


Figure S9a Absorption spectra of the DBASL (50 μ M) in different solvents.

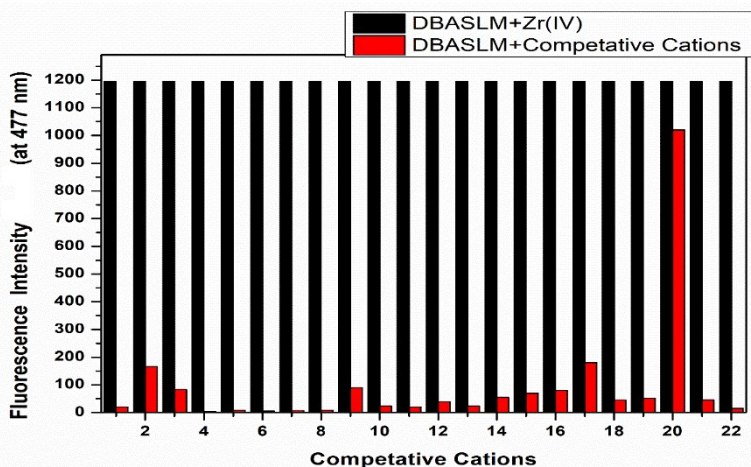


Figure S10 Effect of competitive cations (1300 μM) on the emission intensity of **DBASLM** (50 μM , $\lambda_{\text{ex}} = 278 \text{ nm}$, $\lambda_{\text{em}} = 477 \text{ nm}$) including ZrO^{2+} , K^+ , Al^{3+} , Na^+ , Fe^{2+} , Mg^{2+} , Mn^{2+} , Ni^{2+} , Ca^{2+} , Cd^{2+} , Co^{2+} , Cu^{2+} , Cr^{3+} , Fe^{3+} , Ce^{4+} , Dy^{3+} , Gd^{3+} , Zn^{2+} , La^{3+} , Nd^{3+} , Y^{3+} , Sm^{3+} and H^+ (from left to right, 1-22, EtOH- H_2O , 3:7, v/v)

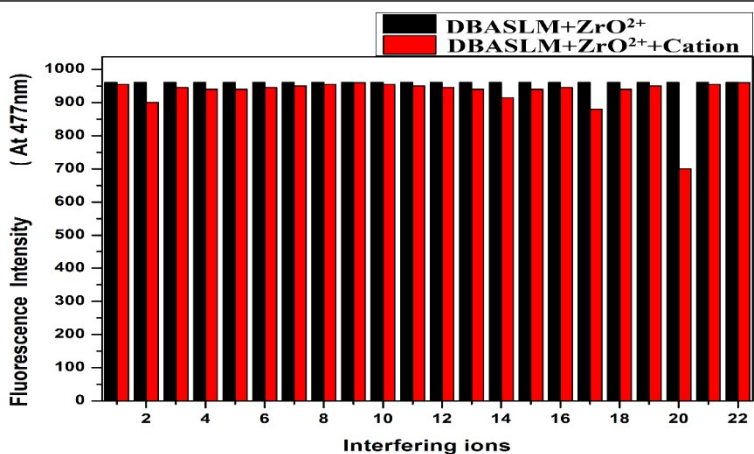


Figure S11 Effect of common tested cations on the emission intensity of **DBASLM** (1500 μM) - ZrO^{2+} (1000 μM) system ($\lambda_{\text{ex}} = 278 \text{ nm}$, $\lambda_{\text{em}} = 477 \text{ nm}$) (K^+ , Al^{3+} , Na^+ , Fe^{2+} , Mg^{2+} , Mn^{2+} , Ni^{2+} , Ca^{2+} , Cd^{2+} , Co^{2+} , Cu^{2+} , Cr^{3+} , Fe^{3+} , Ce^{4+} , Dy^{3+} , Gd^{3+} , Zn^{2+} , La^{3+} , Nd^{3+} , Y^{3+} , Sm^{3+} and H^+ (1-22 from left to right, 1000 μM each in EtOH- H_2O , 3:7, v/v).

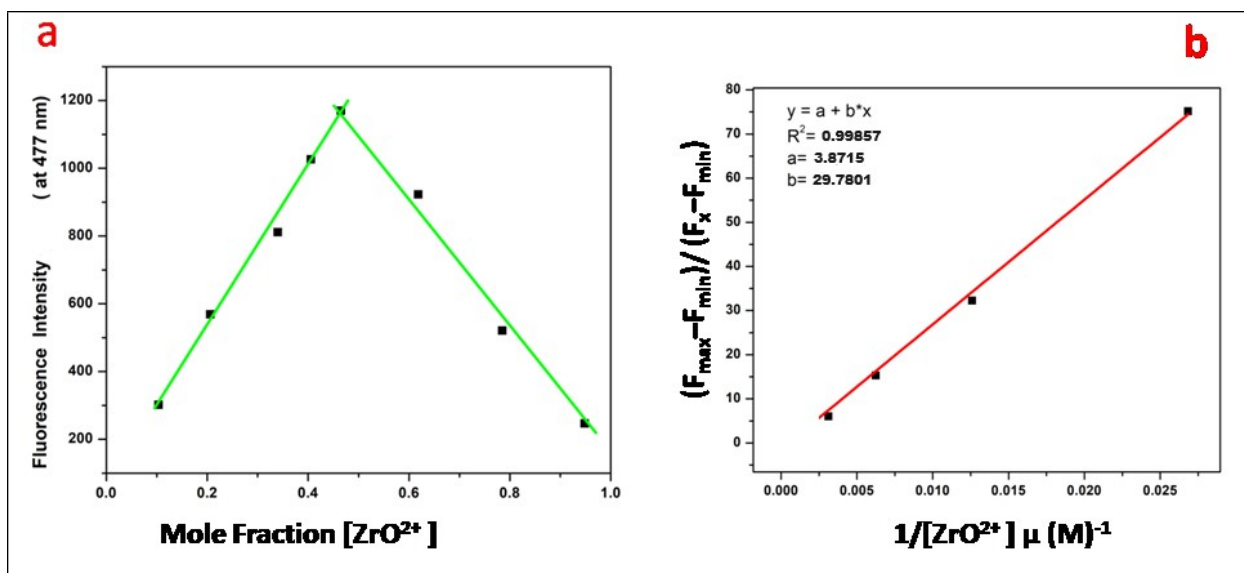


Figure S12 (a) Job's plot for stoichiometry determination of [DBASLM-ZrO²⁺] adduct ($\lambda_{\text{ex}} = 278$ nm, $\lambda_{\text{em}} = 477$ nm, in EtOH-H₂O (3:7, v/v)); (b) determination of association constant of DBASLM with ZrO²⁺ (considering linear portion) ($\lambda_{\text{ex}} = 278$ nm, $\lambda_{\text{em}} = 477$ nm, EtOH-H₂O (3:7, v/v)) using Benesi-Hildebrand method.

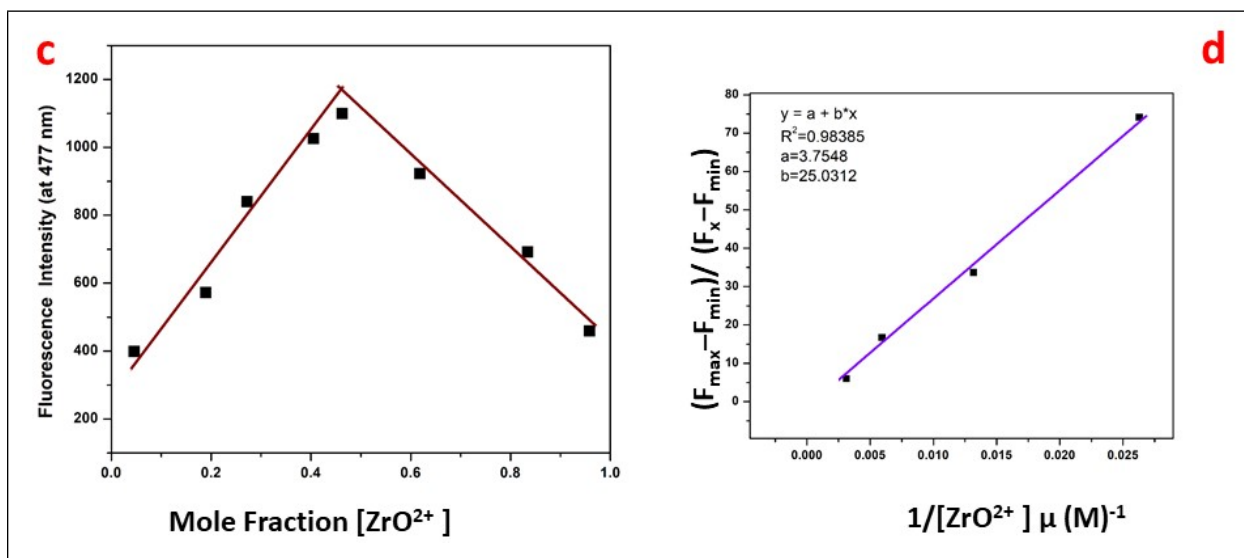


Figure S12 (c) Job's plot for stoichiometry determination of [DBASL-ZrO²⁺] adduct ($\lambda_{\text{ex}} = 278$ nm, $\lambda_{\text{em}} = 477$ nm, in EtOH-H₂O (3:7, v/v)); (d) determination of association constant of DBASL with ZrO²⁺ (considering linear portion) ($\lambda_{\text{ex}} = 278$ nm, $\lambda_{\text{em}} = 477$ nm, EtOH-H₂O (3:7, v/v)) using Benesi-Hildebrand method.

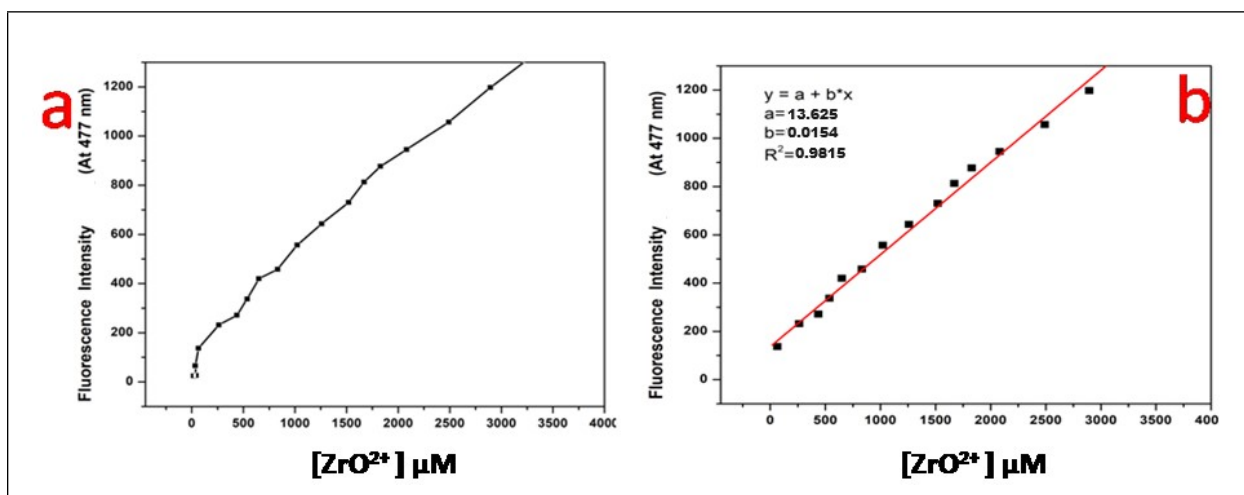


Figure S13 (a) Plot of emission intensities of DBASLM (50 μM) vs. externally added ZrO^{2+} (1.0-3000 μM , EtOH-H₂O (3:7, v/v)) (b) determination of detection limit of ZrO^{2+} using DBASLM (50 μM) ($\lambda_{ex} = 278$ nm, $\lambda_{em} = 477$ nm, EtOH-H₂O (3:7, v/v)) considering linear part of Figure S13a

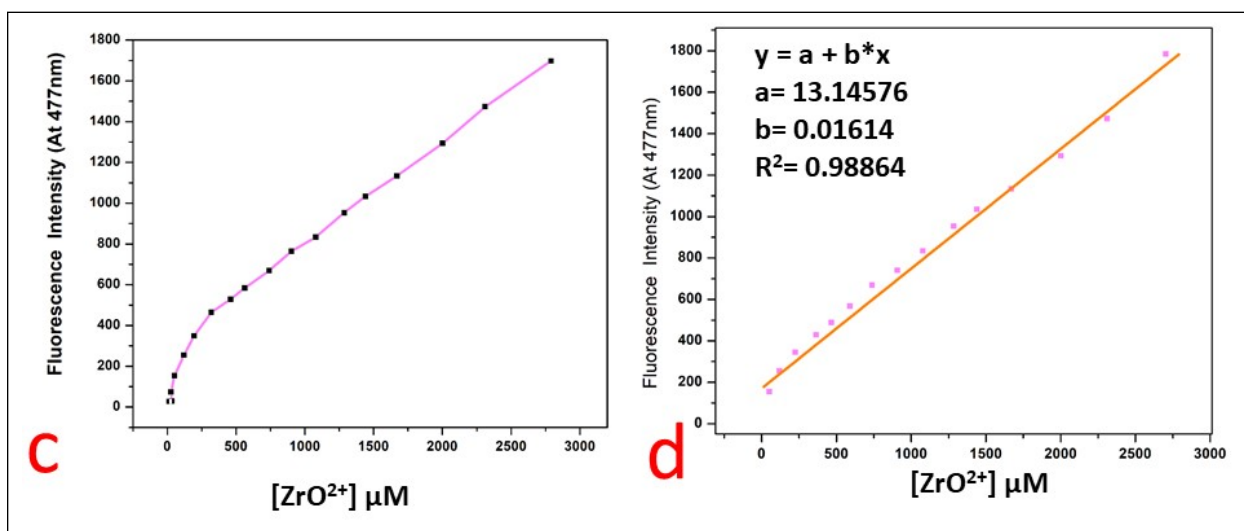


Figure S13 (c) Plot of emission intensities of DBASL (50 μM) vs. externally added ZrO^{2+} (1.0-2800 μM , EtOH-H₂O (3:7, v/v)) (d) determination of detection limit of ZrO^{2+} using DBASL (50 μM) ($\lambda_{ex} = 278$ nm, $\lambda_{em} = 477$ nm, EtOH-H₂O (3:7, v/v)) considering linear part of Figure S13 (c)

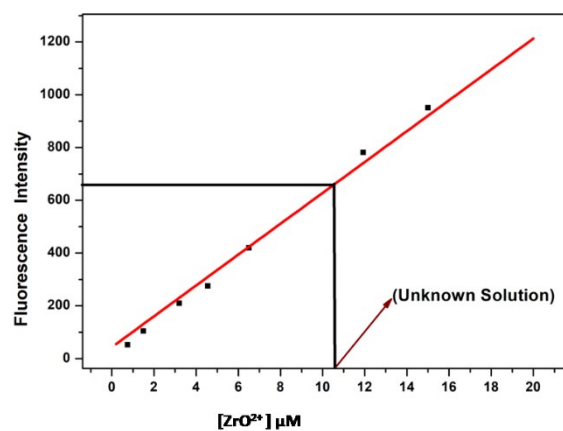


Figure S14 Calibration graph for determination of unknown concentration of ZrO^{2+} employing **DBASLM**

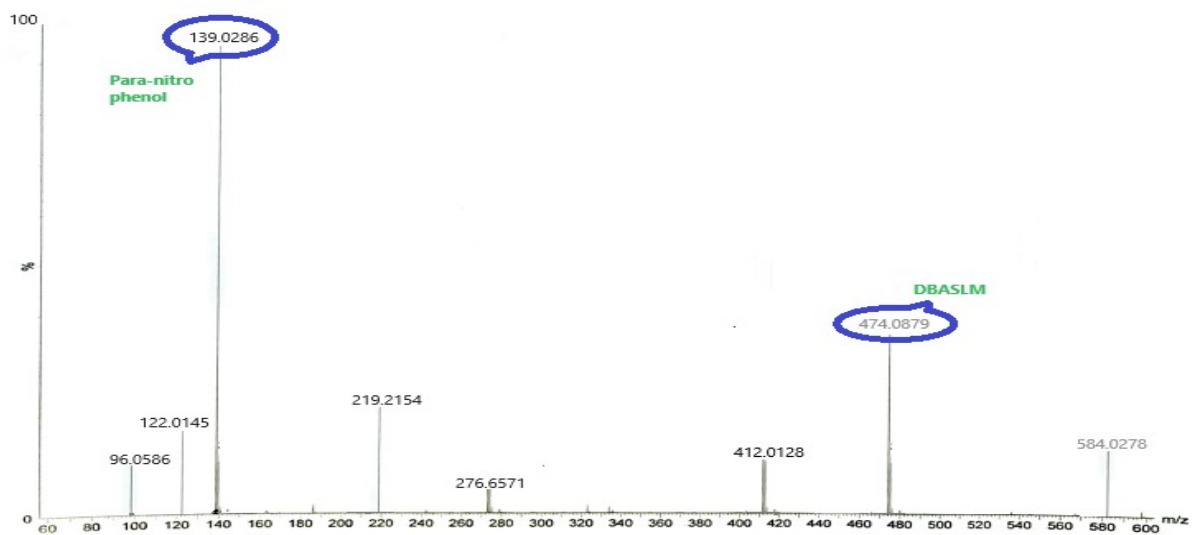


Figure S15 QTOF mass spectrum of $[DBASLM + p\text{-NPP}]$ adduct

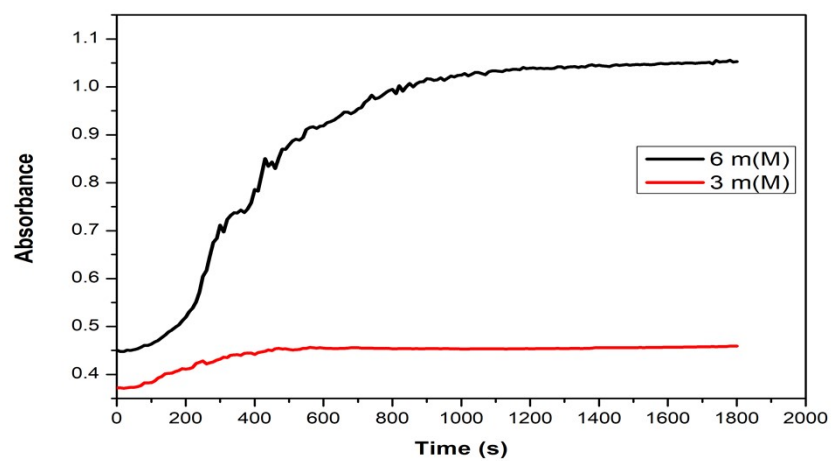


Figure S16 Monitoring of reaction progress between **DBASLM** (0.6 mmol) and ***p*-NPP** using absorption spectroscopy (at 410 nm) in MeOH-H₂O (1:4, v/v, pH 7, PBS buffer)

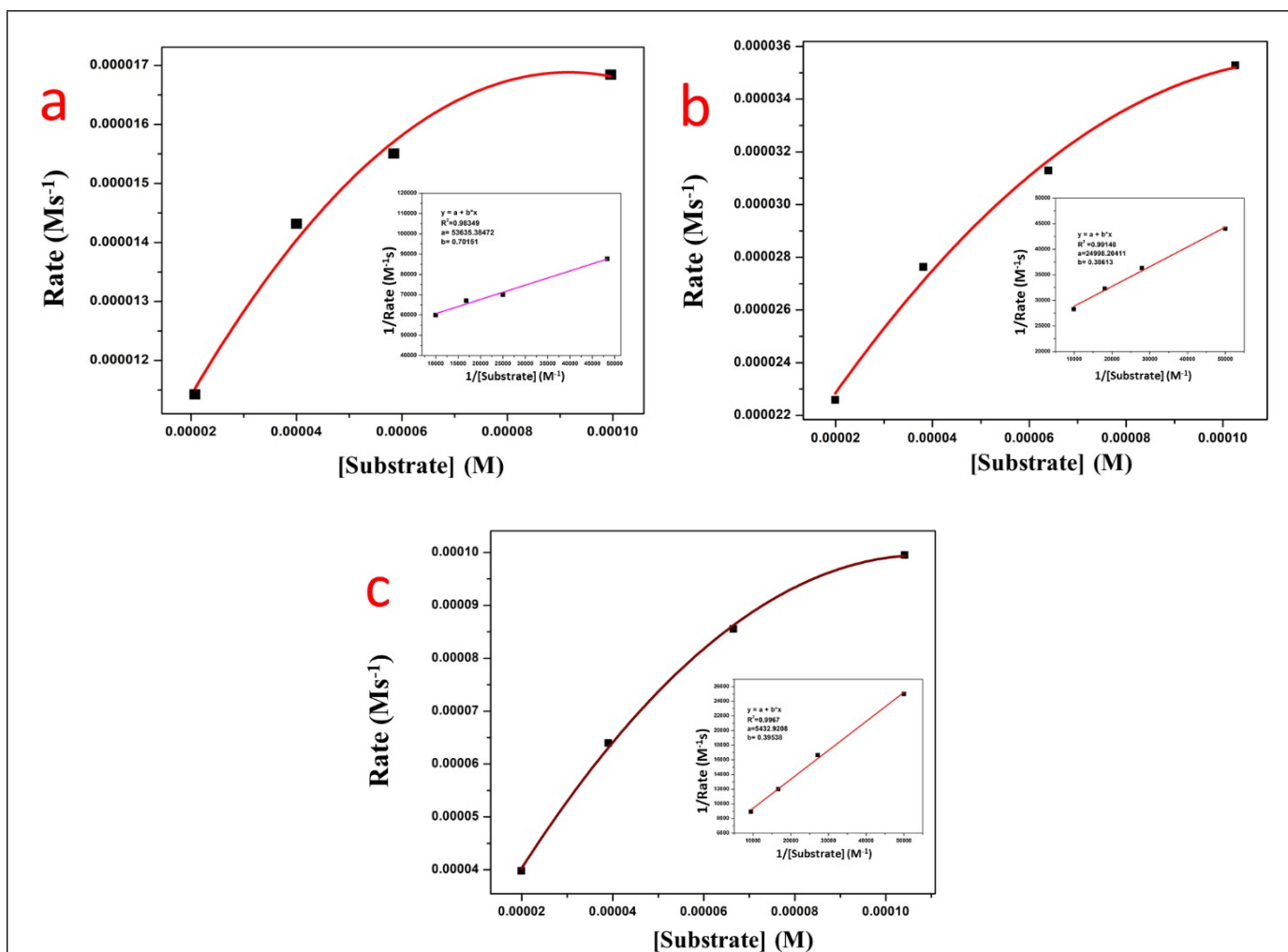


Figure S17 Rate vs. substrate (p -NPP) plot in presence of (a) only solvent, (b) DBASL (0.01 mmol), and (c) DBASLM (0.01 mmol) in MeOH- H_2O (1:4, v/v, pH 7, PBS buffer, 25°C)

Table S1 Summary of crystallographic parameters of DBASLM

Molecules	DBASLM
CCDC	2448883
Empirical formula	$\text{C}_{20}\text{H}_{24}\text{MoN}_4\text{O}_8$
Formula weight	'544.37'
Crystal system	triclinic
Space group-	$P \bar{1}$
Temperature/(K)	200.0(2)

Wavelength/Å	0.71073
a/Å	6.5396(2)
b/Å	12.7039(5)
c/Å	14.4697(4)
α /°	104.639(3)
β /°	93.972(2)
γ /°	101.116(3)
Volume/Å ³	1132.43(7)
Z	2
ρ_{calc} (g/cm ³)	1.597

Table S2 Selected bond lengths [Å] and angles [°] of DBASLM

ATOMS	BOND LENGTH	ATOMS	BOND ANGLE
Mo O3	2.007(2)	O3 Mo O7	149.35(9)
Mo O7	1.932(2)	O3 Mo O4	97.9(1)
Mo O4	1.693(2)	O3 Mo O5	79.04(8)
Mo O5	2.322(2)	O3 Mo O6	98.4(1)
Mo O6	1.711(2)	O3 Mo N2	72.33(9)
Mo N2	2.244(3)	O7 Mo O4	97.9(1)
O3 C1	1.327(3)	O7 Mo O5	81.55(8)
O7 C10	1.360(3)	O7 Mo O6	102.6(1)
O5 C15	1.249(4)	O7 Mo N2	81.36(9)
O2 C7	1.351(3)	O4 Mo O5	171.59(9)
N2 N1	1.392(3)	O4 Mo O6	105.3(1)
N2 C8	1.288(3)	O4 Mo N2	90.7(1)
O1 C5	1.362(3)	O5 Mo O6	82.97(9)
N1 C1	1.307(3)	O5 Mo N2	80.89(8)
N3 C15	1.315(4)	O6 Mo N2	162.6(1)
N3 C16	1.465(5)	Mo O3 C1	119.8(2)

N3 C17	1.465(4)	Mo O7 C10	133.1(2)
C1 C2	1.465(4)	Mo O5 C15	131.4(2)
C8 C9	1.448(4)	Mo N2 N1	114.7(2)
C10 C9	1.407(5)	Mo N2 C8	127.7(2)
C10 C11	1.395(4)	N1 N2 C8	117.0(2)
C2 C3	1.401(4)	N2 N1 C1	110.6(2)
C2 C7	1.417(5)	C15 N3 C16	121.3(3)
C3 C4	1.379(4)	C15 N3 C17	121.4(3)
C7 C6	1.389(4)	C16 N3 C17	117.3(3)
C9 C14	1.409(4)	O3 C1 N1	122.5(3)
C6 C5	1.386(4)	O3 C1 C2	118.1(2)
C14 C13	1.379(5)	N1 C1 C2	119.4(2)
C5 C4	1.399(5)	N2 C8 C9	123.4(3)
C11 C12	1.386(5)	H8 C8 C9	118.3(3)
C13 C12	1.382(6)	O7 C10 C9	122.4(3)
N4 C18	1.324(5)	O7 C10 C11	117.7(3)
N4 C19	1.454(5)	C9 C10 C11	119.9(3)
N4 C20	1.440(7)	O5 C15 N3	123.8(3)
O8 C18	1.230(6)	C1 C2 C3	120.1(3)
C8 H8	0.930	C1 C2 C7	121.6(3)
		C3 C2 C7	118.3(3)
		C2 C3 C4	121.9(3)
		O2 C7 C2	123.4(3)
		O2 C7 C6	116.8(3)
		C2 C7 C6	119.8(3)
		C8 C9 C10	123.5(3)
		C8 C9 C14	117.9(3)
		C10 C9 C14	118.6(3)
		C7 C6 C5	120.5(3)
		C9 C14 C13	120.7(3)

		O1 C5 C6	121.8(3)
		O1 C5 C4	117.7(3)
		C6 C5 C4	120.6(3)
		C3 C4 C5	118.9(3)
		C10 C11 C12	120.2(3)
		C14 C13 C12	120.2(4)
		C11 C12 C13	120.4(4)
		C18 N4 C19	122.0(3)
		C18 N4 C20	120.7(3)
		C19 N4 C20	117.2(3)
		N4 C18 O8	124.4(4)

Table S3 Results of TD-DFT studies on **DBASLM** and **DBASLZ**

Compound	Electronic Transitions	Energy (eV)	Wavelength (nm)	f^b	Transitions involved
DBASLM	$S_0 \rightarrow S_1$	2.9181 eV	424.88 nm	$f^b = 0.1877$	HOMO-1 \rightarrow LUMO HOMO \rightarrow LUMO
	$S_0 \rightarrow S_2$	3.4227 eV	362.24 nm	$f^b = 0.0635$	HOMO-1 \rightarrow LUMO HOMO \rightarrow LUMO
	$S_0 \rightarrow S_3$	3.4640 eV	357.92 nm	$f^b = 0.0259$	HOMO-2 \rightarrow LUMO HOMO-1 \rightarrow LUMO+1 HOMO \rightarrow LUMO+1 HOMO \rightarrow LUMO+2
DBASLZ	$S_0 \rightarrow S_1$	3.0738 eV	403.35 nm	$f^b = 0.0036$	HOMO-1 \rightarrow LUMO HOMO \rightarrow LUMO HOMO \rightarrow LUMO+1
	$S_0 \rightarrow S_2$	3.3105 eV	374.52 nm	$f^b = 0.5330$	HOMO \rightarrow LUMO HOMO \rightarrow LUMO+1

	S₀→S₃	3.5804 eV	346.28 nm	f^b = 0.0011	HOMO-3→LUMO HOMO-2→LUMO HOMO-1→LUMO HOMO→LUMO
--	------------------------------------	------------------	------------------	-------------------------------	------------------------------------------------------------------------------------

f^b = oscillator strength (f) for band or transition b.¹⁰

f^b value	Transition type
0.5 – 1.0	Strong $\pi \rightarrow \pi^*$ (Intense UV–vis band)
0.1 – 0.5	Medium $\pi \rightarrow \pi^*$ (Moderate absorption)
< 0.05	$n \rightarrow \pi^*$ or forbidden (weak or nearly dark transition)

Reference

10. M. Kaupp, M. B. et al., Computational Molecular Spectroscopy, Wiley, 2012.